

4*f*-shell configuration of Yb in InP studied by electron spin resonance

T. Ishiyama^{a)} and K. Murakami

Institute of Materials Science, University of Tsukuba, 1-1-1 Tennoudai, Tsukuba, Ibaraki 305, Japan

K. Takahei and A. Taguchi

NTT Basic Research Laboratories, 3-1 Morinosato-Wakamiya, Atsugi, Kanagawa 243-01, Japan

(Received 24 March 1997; accepted for publication 21 July 1997)

We have performed electron spin resonance (ESR) measurements on Yb-doped *n*-type and *p*-type InP layers epitaxially grown by metalorganic chemical vapor deposition. ESR spectra of Yb³⁺(4*f*¹³) were observed in both *n*-type and *p*-type samples. However, the ESR intensity of Yb³⁺(4*f*¹³) for *n*-type samples was found to be much lower than that for *p*-type samples. This suggests that most Yb ions in Yb-doped *n*-type InP are in the Yb²⁺(4*f*¹⁴) state rather than in the Yb³⁺(4*f*¹³) state. Thus an electron captured by the trap level formed by Yb in the band gap of InP is not located outside the Yb 4*f* shell as reported previously, but accommodated in the Yb 4*f* shell.

© 1997 American Institute of Physics. [S0021-8979(97)01821-5]

I. INTRODUCTION

Semiconductors doped with rare earth (RE) impurities have attracted much attention because of their possible applications to new optical devices, as those semiconductors exhibit sharp and temperature-stable luminescence. The luminescence mechanism and the atomic configuration of RE impurities in semiconductor hosts have been widely studied. Among many possible combinations of RE impurities and semiconductor hosts, Yb impurities incorporated in InP have been one of the most extensively studied, because Yb-doped InP has two characteristic properties, as follows. The first is that its Yb intra-4*f*-shell photoluminescence spectrum does not depend on sample preparation methods, indicating the Yb forms only one kind of light-emitting center in InP.¹ It has been shown that the Yb substitutes for In and the Yb³⁺(4*f*¹³) is the luminescence center of the tetrahedral symmetry.² The second is that the energy level scheme of the Yb 4*f* shell is simple, having only one spin-orbit split excited state.

Initially, it was proposed that the acceptor level Yb³⁺/Yb²⁺ would be in the lower half of the band gap of InP, since Yb-doped InP grown by liquid-phase epitaxy (LPE) showed *p*-type conductivity.^{3,4} However, it was revealed that the *p*-type behavior of LPE-grown materials could be due to unintentionally doped shallow acceptor impurities.⁵ Later, deep level transient spectroscopy (DLTS)⁶ and Hall effect measurement^{6,7} revealed that Yb forms an acceptorlike electron trap (AE trap) level at 30 meV below the bottom of the conduction band. The AE trap does not contribute carriers by itself, but it can capture an electron and become negatively charged. Whether the electron captured by AE trap is accommodated in the Yb 4*f* shell or not is related to the mechanism and magnitude of the interaction between the Yb 4*f* shell and InP host. This is a very important issue concerning the Yb 4*f*-shell excitation process.

Yb³⁺(4*f*¹³) in InP is electron spin resonance (ESR) active, while Yb²⁺(4*f*¹⁴) with a closed 4*f* shell is ESR inactive. Lambert *et al.*^{7,8} observed an ESR spectrum from unin-

tionally Si doped *n*-type bulk InP and concluded that Yb ions are in the Yb³⁺(4*f*¹³) state rather than the Yb²⁺(4*f*¹⁴) state even in *n*-type InP. On the basis of their results, it has been recognized that the electron captured by the AE trap is located outside the 4*f* shell and that Yb ions are in the Yb³⁺(4*f*¹³) state. However, the *n*-type bulk InP sample used in their study was doped only unintentionally from a silica crucible and there could have been a significant degree of inhomogeneity in the donor concentration. Therefore, it is worth reexamining the 4*f*-shell configuration of Yb ions by investigating the relation between the ESR signal intensity of Yb³⁺(4*f*¹³) and the carrier concentration in well-controlled epitaxial *p*- and *n*-type Yb-doped InP layers.

In this study, ESR measurements were performed on *n*-type and *p*-type Yb-doped InP epitaxial layers grown by metalorganic chemical vapor deposition (MOCVD). In contrast to the results reported by Lambert *et al.*,^{7,8} the ESR intensity of Yb³⁺(4*f*¹³) for *n*-type samples was found to be much lower than that for *p*-type samples, indicating that an electron captured by the AE trap is accommodated in the Yb 4*f* shell and the Yb ion is in the Yb²⁺(4*f*¹⁴) state.

II. EXPERIMENTAL PROCEDURES

The Yb-doped InP samples used in this study, which had various Yb concentrations and carrier concentrations, were grown on (100)-oriented Fe-doped semi-insulating InP substrates by MOCVD, using tris(cyclopentadienyl)ytterbium as a Yb source. The thickness of the grown epitaxial layers was in the range of 1–5 μm. Nominally undoped samples showed *n*-type conductivity. H₂Se and tri-ethyl Zn were used as *n*- and *p*-type doping sources, respectively. Doping concentration profiles of Yb, Se, and Zn were measured by secondary-ion mass spectroscopy (SIMS) and carrier concentrations were determined by Hall measurements. The Yb, Se, Zn, and carrier concentrations in the samples are listed in Table I. The samples were grown at various temperatures (Table I), but the effects of the growth temperature will not be discussed in this article, as it contributed only a minor change to the ESR activity of the Yb atoms. The photoluminescence (PL) spectra were measured at 5 K, using a He–Ne

^{a)}Electronic mail: T.I.@ims.tsukuba.ac.jp

TABLE I. Yb, Se, and Zn concentrations and electrical characteristics of samples.

Sample	Yb concentration ($\times 10^{17}/\text{cm}^3$)	Se or Zn concentration ($\times 10^{17}/\text{cm}^3$)	Conductivity type	Carrier concentration at 300 K ($\times 10^{17}/\text{cm}^3$)	Growth temperature ($^\circ\text{C}$)
1	4.0	Zn~6	<i>p</i>	5.6	640
2	6.0	Zn<4	<i>p</i>	1.8	640
3	19.0	No	<i>n</i>	0.09	560
4	4.5	No	<i>n</i>	0.16	600
5	10.0	No	<i>n</i>	0.19	640
6	2.8	Se 2.1	<i>n</i>	1.6	600
7	No	Se 9.0	<i>n</i>	6.7	600

laser operating at 632.8 nm as a source of excitation light. ESR measurements were performed at 4.2 K with an X-band (9.05 GHz) spectrometer. The relative ESR intensity of $\text{Yb}^{3+}(4f^{13})$ was obtained by using an ESR signal of Mn^{2+} in MgO measured simultaneously. The magnetic field was swept from 500 to 13 500 G. The effective *g* value obtained in this range of the magnetic field is from 0.5 to 16.

III. EXPERIMENTAL RESULTS AND DISCUSSION

ESR spectra for $\text{Yb}^{3+}(4f^{13})$ in Yb- and Zn-doped *p*-type sample 1 and Yb- and Se-doped *n*-type sample 6 are shown

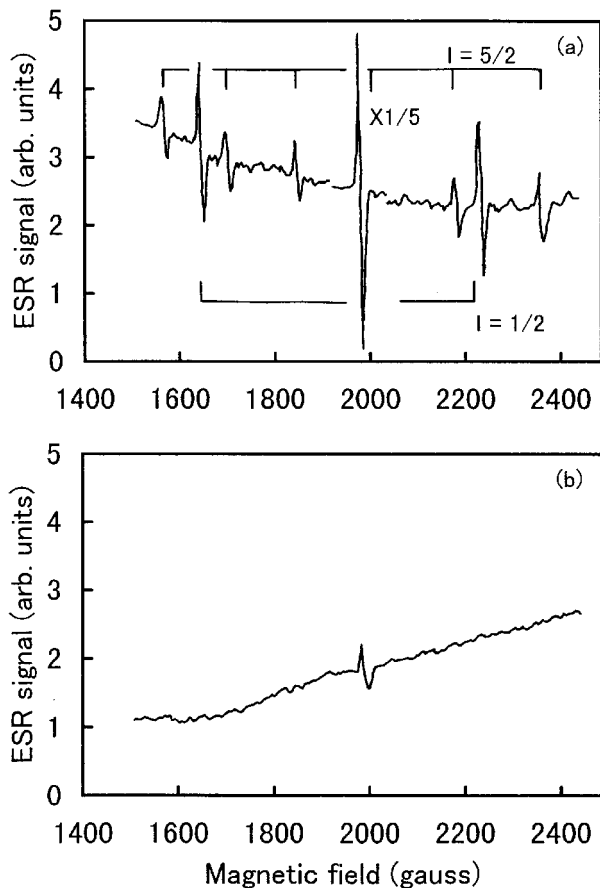


FIG. 1. Typical ESR spectra of $\text{Yb}^{3+}(4f^{13})$ in (a) the Yb- and Zn-doped *p*-type sample 1 and (b) the Yb- and Se-doped *n*-type sample 6. These are recorded at 4.2 K and 9.05 GHz.

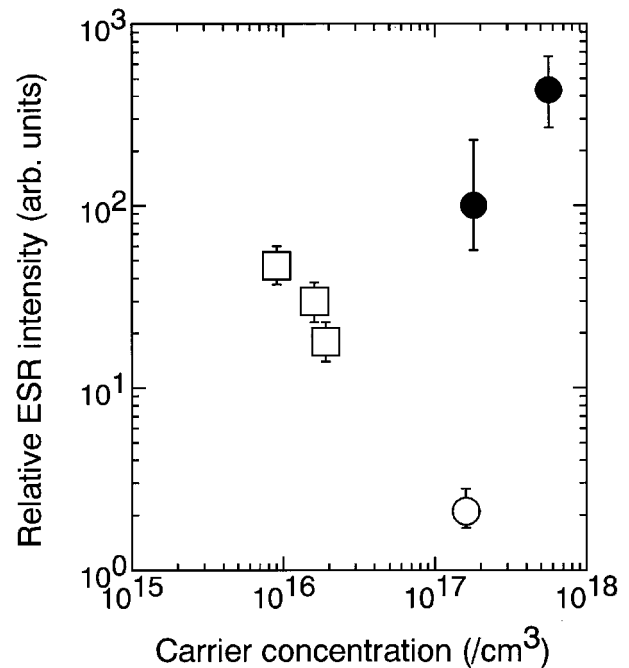


FIG. 2. Relative ESR intensity of $\text{Yb}^{3+}(4f^{13})$ for nominally undoped *n*-type (\square), Se-doped *n*-type (\circ) and Zn-doped *p*-type (\bullet) samples as a function of the carrier concentration. The relative ESR intensity was normalized by the number of Yb atoms in the epitaxial layer measured by SIMS. The errors in the relative ESR intensity are mainly due to nonuniformity of Yb concentrations in the epitaxial layers.

in Figs. 1(a) and 1(b), respectively. The ESR spectra are isotropic. The spectrum of *p*-type InP consists of a strong central line due to the isotopes of Yb with a nuclear spin of zero ($I=0$, 69.4%), two hyperfine structure lines due to ^{171}Yb ($I=1/2$, 14.4%), and six hyperfine structure lines due to ^{173}Yb ($I=5/2$, 16.2%), as shown in Fig. 1(a). However, the hyperfine structure lines do not appear in *n*-type sample 6, as shown in Fig. 1(b). This is because of the much lower ESR intensity of $\text{Yb}^{3+}(4f^{13})$ for sample 6 than that for sample 1. The effective *g* value of $\text{Yb}^{3+}(4f^{13})$ is identical for *n*-type and *p*-type samples, $g=3.293\pm 0.001$. This *g* value is comparable to previously reported values of 3.29^8 and 3.291 ± 0.001^9 by ESR and 3.0 ± 0.1^2 by Zeeman spectroscopy.

If an electron captured by the AE trap is located outside the Yb 4*f* shell, a change in the crystal field is expected, yielding a *g* value of $\text{Yb}^{3+}(4f^{13})$ different from the *g* value of $\text{Yb}^{3+}(4f^{13})$ without an electron. However, the *g* value of $\text{Yb}^{3+}(4f^{13})$ in the *n*-type sample is identical with that in the *p*-type sample. This suggests that the Yb centers responsible for the ESR signals of *n*- and *p*-type samples are identical. We will first discuss the reduction in the ESR intensity for the *n*-type samples and then discuss the origin of weak ESR signals for the *n*-type samples.

Figure 2 shows the relative ESR intensity of $\text{Yb}^{3+}(4f^{13})$ normalized by the number of Yb atoms in the epitaxial layers as a function of the carrier concentration. The numbers of Yb atoms in epitaxial layers were estimated from the Yb concentration profiles measured by SIMS. The relative ESR intensities for the *n*-type samples (\circ, \square) decrease with increas-

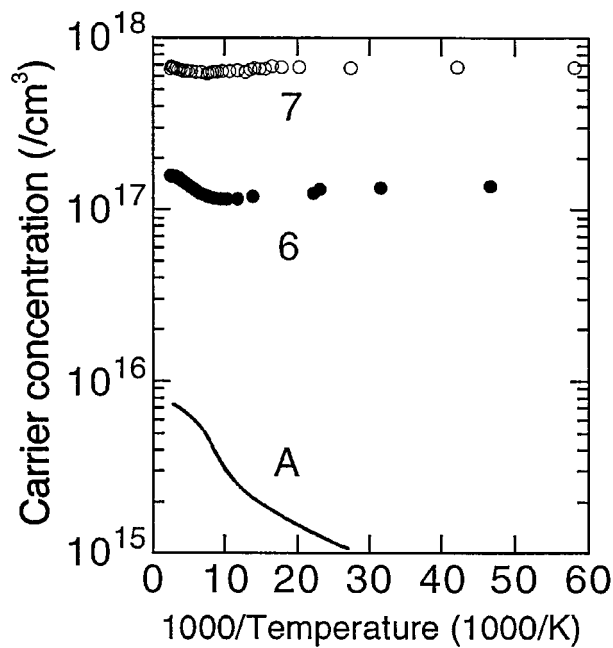


FIG. 3. Temperature dependence of the carrier concentration obtained by Hall measurement for the Yb- and Se-doped sample 6 (●) and the Se-doped sample 7 (○). The data for Yb-doped sample A were taken from Ref. 5.

ing the carrier concentration and are lower than those for the *p*-type samples (●). In the Se-doped sample (○) having a very high carrier concentration, the relative ESR intensity is two orders of magnitude lower than that for *p*-type samples. Because a $\text{Yb}^{2+}(4f^{14})$ ion with a closed $4f$ shell is ESR inactive, these results suggest that the donor electron captured by the AE trap is accommodated in the $4f$ shell and that the Yb ion in *n*-type Yb-doped InP is in the $\text{Yb}^{2+}(4f^{14})$ state. However, there is a possibility that the large decrease in the ESR intensity, i.e., the number of $\text{Yb}^{3+}(4f^{13})$ ions, is caused by the formation of ESR-inactive complexes of Yb and Se in the Yb- and Se-doped *n*-type sample 6. If Yb–Se complex centers are efficiently formed, we should observe the decrease in the concentration of the AE trap formed by Yb.

In order to investigate this possibility, the AE trap concentration in Yb- and Se-doped sample 6 was estimated by measuring the temperature dependence of the carrier concentration. Figure 3 shows the temperature dependence of the carrier concentration for the Yb- and Se-doped sample 6 and Se-doped sample 7. The solid line in Fig. 3 shows the result for the MOCVD-grown sample A doped with Yb ($1 \times 10^{16}/\text{cm}^3$) and a low concentration of residual donor, which is taken from Ref. 6. Yb in InP forms an AE trap level at 30 meV below the bottom of the conduction band. The temperature dependence of the carrier concentration for Yb- and Se-doped *n*-type samples 6 and A shows an increase in carrier concentration above about 77 K (below $1000/T \sim 13$). This is because in both samples the electron captured by the AE trap was excited to the conduction band. The carrier concentration of Se-doped sample 7 without Yb does not depend on temperature in the same temperature range, in contrast to the result with the Yb- and Se-doped sample. The

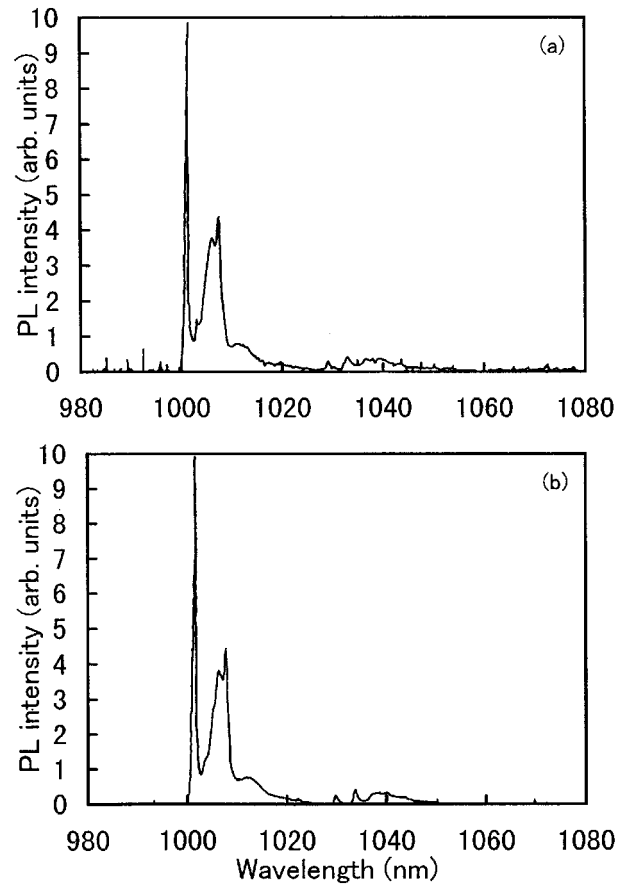


FIG. 4. PL spectra at 5 K for (a) the Yb- and Se-doped *n*-type sample 6 and (b) the Yb- and Zn-doped *p*-type sample 2.

AE trap concentration measured by DLTS was evaluated to be about a quarter of the Yb concentration in the sample measured by SIMS in the present Yb concentration range,⁶ and the carrier concentration increase above ~ 77 K corresponds to the AE trap concentration. In sample 6, the increment of the carrier concentration above ~ 77 K was estimated to be approximately $0.5 \times 10^{17}/\text{cm}^3$; this value is nearly equal to a quarter of Yb concentration, $2.8 \times 10^{17}/\text{cm}^3$. Therefore, it is likely that most of the Yb ions do not form complexes with Se in sample 6.

Another argument against the formation of Yb–Se complexes is that the Yb and Se concentrations ($\sim 10^{17}/\text{cm}^3$) in sample 6 are relatively low, so that efficient complex formation is not expected during MOCVD growth. PL spectra at 5 K for the Yb- and Se-doped *n*-type sample 6 and *p*-type sample 2 are shown in Figs. 4(a) and 4(b). The PL spectrum for sample 6 exhibits a structure identical to that for sample 2. This shows that a Yb-related luminescence center different from that in *p*-type samples is not formed in *n*-type samples. All these experimental results suggest that the very low ESR intensity of $\text{Yb}^{3+}(4f^{13})$ observed for sample 6 is not due to the formation of Yb–Se complexes.

The relatively low ESR intensities of $\text{Yb}^{3+}(4f^{13})$ for the *n*-type samples compared to those for the *p*-type samples indicate that the donor electron captured by the AE trap is accommodated in the $4f$ shell and that most Yb ions in Yb-

doped *n*-type InP are in the $\text{Yb}^{2+}(4f^{14})$ state rather than in the $\text{Yb}^{3+}(4f^{13})$ state. In sample 6, which has a higher donor concentration than the AE trap concentration (that is, about a quarter of the Yb concentration), there should be no ESR signals. However, a very weak ESR signal of $\text{Yb}^{3+}(4f^{13})$ was observed even in sample 6. It is likely that the weak ESR signal comes from Yb impurities in the depletion layer near the surface.

It has been believed that the electron captured by the AE trap is not accommodated in the *4f* shell, but instead is located outside the *4f* shell. This model was based on the fact that Lambert *et al.*^{7,8} observed an ESR signal of $\text{Yb}^{3+}(4f^{13})$ even in Yb-doped *n*-type InP, which has a higher concentration of carrier than of Yb. However, the samples used in their study were melt-grown crystals with *n*-type impurities incorporated from a silica crucible. Thus there could be an inhomogeneity in the samples. That is, to show an ESR signal of $\text{Yb}^{3+}(4f^{13})$, the carrier concentration in some parts of the sample may have been lower than the AE trap concentration.

The energy transfer probability between the host and RE *4f* shell is estimated to be much larger for Yb doped InP than for other RE doped semiconductors.¹⁰ This may be related to the fact that the electron captured by the AE trap is accommodated in Yb *4f* shell to change from $\text{Yb}^{3+}(4f^{13})$ state to $\text{Yb}^{2+}(4f^{14})$ state, whereas other rare earth elements such as Er and Nd take stable trivalent states. These suggest

that the interaction between Yb *4f* shell and InP host is strong.

IV. CONCLUSIONS

ESR measurements have been performed on Yb-doped *n*-type and *p*-type InP grown by MOCVD. It was found that the ESR intensity of $\text{Yb}^{3+}(4f^{13})$ for the *n*-type samples is two orders of magnitude lower than that for the *p*-type samples. This indicates that the donor electron captured by AE trap is accommodated in the Yb *4f* shell and thus most Yb ions in *n*-type InP are in the $\text{Yb}^{2+}(4f^{14})$ state.

¹W. Korber, J. Weber, A. Hangleiter, K. W. Benz, H. Ennen, and H. D. Muller, *J. Cryst. Growth* **79**, 741 (1986).

²G. Aszodi, J. Weber, Ch. Uihlein, L. Pu-lin, H. Ennen, U. Kaufmann, J. Schneider, and J. Windscheif, *Phys. Rev. B* **31**, 7767 (1985).

³W. Korber and A. Hangleiter, *Appl. Phys. Lett.* **52**, 114 (1988).

⁴P. B. Klein, *Solid State Commun.* **65**, 1097 (1988).

⁵H. Nakagome, K. Takahei, and Y. Honma, *J. Cryst. Growth* **85**, 345 (1987).

⁶P. S. Whitney, K. Uwai, H. Nakagome, and K. Takahei, *Appl. Phys. Lett.* **53**, 2074 (1988).

⁷B. Lambert, A. Le Corre, Y. Toudic, C. Lhomer, G. Grandpierre, and M. Gauneau, *J. Phys.: Condens. Matter* **2**, 479 (1990).

⁸B. Lambert, Y. Toudic, G. Grandpierre, A. Rupert, and A. Le Corre, *Electron. Lett.* **24**, 1446 (1988).

⁹V. F. Masterov, V. V. Romanov, and K. F. Shtel'makh, *Sov. Phys. Solid State* **25**, 824 (1983).

¹⁰A. Taguchi and K. Takahei, *J. Appl. Phys.* **79**, 4330 (1996).